

## Transfer Reaction Studies with Exotic Nuclei

W.N. Catford<sup>1</sup>, R.C. Lemmon<sup>2</sup>, C.N. Timis<sup>1</sup>, M. Labiche<sup>3</sup>, L. Caballero<sup>4</sup>  
and R. Chapman<sup>3</sup>

<sup>1</sup> *University of Surrey, Guildford, Surrey GU2 7XH, UK*

<sup>2</sup> *CCLRC Daresbury Laboratory, Warrington, Cheshire WA4 4AD, UK*

<sup>3</sup> *University of Paisley, Paisley, Scotland PA1 2BE, UK*

<sup>4</sup> *IFIC, CSIC/University of Valencia, Valencia E-46071, Spain*

**Abstract.** Transfer reactions offer the possibility to study single-particle structure in exotic nuclei, including the structure of ground states, the structure of excited states, and the location and distribution of single particle strength. The last of these means that the evolution of single particle orbitals away from stability, and the consequent changes in shell structure and collectivity, can be studied in detail. The kinematics of transfer reactions initiated by protons and deuterons, in inverse kinematics, have characteristic features that mean a general-purpose design of array can be applied to a wide range of experiments. Due to resolution considerations, coincident gamma-ray detection is highly desirable or even essential. A new silicon detector array called TIARA has been designed so that it can be used together with the segmented germanium detectors of the EXOGAM array. The setup for TIARA is now complete, having been built by several UK groups, and it was recently commissioned by the extended UK-France-Spain collaboration at GANIL. The EXOGAM gamma-ray detectors can be placed as close as 50mm to the target, covering  $2/3$  of  $4\pi$ , so as to give the maximum detection efficiency. Simultaneously, the VAMOS magnetic spectrometer can be coupled to the system at zero degrees, to separate the beam from reaction products and give precise energy and angle measurements. The features of TIARA, as presently installed, are described.

### THE PROMISE OF TRANSFER REACTIONS

Transfer reactions initiated by light ions are well established, through experiments over many years using stable beams, as a clear probe of single particle structure in nuclei [1-4]. In particular, transfer reactions in which a single nucleon is transferred between the beam and target particles can allow the orbital angular momentum in single-particle states to be deduced. This, together with the excitation energies of the levels involved, and the extent to which they exhaust the full single particle strength (i.e. the spectroscopic factor), are the main properties to be measured. In the future, in experiments using radioactive beams, transfer reactions again promise to be a rich source of information concerning single-particle energy levels and the precise shell model structure of nuclei far from stability. Typical experiments for transfer are performed at collision energies of order 10 MeV/A. Transfer reactions initiated by heavy ions ( ${}^6\text{Li}$  and heavier) are also established as useful spectroscopic tools. In the peripheral collisions of heavy ions at these energies, an additional strong selectivity is observed [5] that allows the spin of the final orbital to be deduced, in terms of whether it is  $j = \ell + 1/2$  or  $j = \ell - 1/2$ . This follows from conservation of linear and angular

momentum for the system including the transferred nucleon, plus angular momentum selection and combination rules [6]. In studies of exotic nuclei (see for example [7]) this selectivity has allowed the spins of levels to be identified with some confidence, even when the yield is too low to measure an angular distribution.

For studies of ground states of very exotic nuclei, a complementary technique has been developed that allows the orbitals populated by valence nucleons to be deduced, along with their occupancy, or spectroscopic factor. The process of single-nucleon knockout is found to have a cross section of one to two orders of magnitude higher than the typical 1-10 mb/sr cross section of a transfer reaction populating a reasonably strong single-particle state. The simple picture of the sudden removal of a nucleon from its valence orbital, which is employed in the analysis of knockout, works rather well at energies of order 100 MeV/A [8,9]. Because the core survives in these experiments, and is detected at very forward angles, very peripheral collisions are automatically selected. During these collisions, if the target nucleus is imagined as a black disk, a “hole” is bored out of the wavefunction of the valence nucleon. In other words, for the valence nucleon to be removed, only a certain part of its wavefunction will be involved – namely, the part that extends beyond the core and overlaps with the black disk. The angular momentum content of this part of the wavefunction can be computed. The removal of this angular momentum affects in turn the magnetic substate population of the surviving core and hence its longitudinal momentum. The result is that high-resolution measurements of the core momentum (using a magnetic spectrometer typically, but not necessarily) can reveal the angular momentum of the removed nucleon. An elegant example of this type of analysis is an experiment [10] using a “cocktail beam” of many different species, which shows the change in angular momentum of the valence nucleons for nuclei across a range of the nuclear chart. From this brief description, it is evident that knockout will be particularly effective when the valence nucleons are weakly bound, because then the wavefunction will typically extend significantly beyond the core. Thus, knockout as a spectroscopic technique is especially valuable to study nuclei near the drip-line, where simultaneously the reaction mechanism is at its most pure and the cross sections highest. For the removal of nucleons that are more tightly bound, the cross sections become closer to those for transfer.

An interesting feature of transfer reactions such as (d,p) or ( $\alpha$ , $^3\text{He}$ ) is that a neutron can be added to a neutron-rich projectile to make states in a nucleus even further from stability. Ideally, spins and spectroscopic factors of various states will be measured, along with their excitation energies. It is sometimes the case, however, that the relative spectroscopic factors of different final states in a given reaction can be extracted with more confidence than the absolute values. Even in the cases where the absolute values are not so well defined, the transfer data will clearly indicate the nature and energies of the states with the strongest single-particle character, and this is itself very valuable information to have. The exploitation of (d,p) reactions looks to be a particularly important area for future work with radioactive beams.

Single particle levels are of interest close to closed shells because they can be used to fix the parameters for shell model calculations and also to test the predictions. However, it should not be forgotten that transfer can also be an important tool to study deformed nuclei. If a deformed nucleus has a single valence particle in a particular

Nilsson orbital, the wavefunction of that nucleon can be expanded in terms of a basis comprising the spherical shell model orbitals in the parent shell:  $|\psi\rangle = \sum_j c_j |j\rangle$  where the  $|j\rangle$  represent the spherical orbitals with good angular momentum quantum number,  $j$ . If a single-nucleon transfer reaction is performed using a target of the even-even core nucleus, then the band in the deformed product is populated by the transferred nucleon entering the Nilsson orbital  $|\psi\rangle$ . The state in the band that has spin  $j$  can only be formed (at least, in a single-step transfer) via the component  $|j\rangle$  of the expansion of the Nilsson orbital, and the magnitude of the cross section will reflect the magnitude of the coefficient  $c_j$ . In the sense that the set of coefficients  $c_j$  can be thought of as a sort of DNA (or actual) fingerprint of the Nilsson orbital, the relative populations in transfer, of the various states in a rotational band, represent a fingerprint that identifies the orbital on which the band is built. Knowing this orbital can, in turn, allow the deformation to be inferred. This application of transfer reactions is discussed by Bohr and Mottelson [11] and reviewed extensively in ref. [12].

## **SPECIFIC ISSUES CONCERNING TRANSFER WITH RADIOACTIVE BEAMS**

### **What has been done with radioactive beams**

The literature of transfer experiments which use radioactive beams to perform nuclear spectroscopy, exploiting the otherwise traditional methods of angular distribution measurements, is growing. Amongst the first were a measurement of the astrophysically interesting  $^{56}\text{Ni}(d,p)^{57}\text{Ni}$  reaction [13] using a beam of radioactive  $^{56}\text{Ni}$  ions accelerated in the Argonne tandem, and a measurement of the structure of the halo nucleus  $^{11}\text{Be}$  via the  $^{11}\text{Be}(p,d)^{10}\text{Be}$  reaction [14,15] using a secondary beam produced at GANIL by fragmentation. Because  $^{10}\text{Be}$  is rather collective, multistep reactions needed to be considered in the  $^{11}\text{Be}$  case, in a full theoretical treatment [15]. Together with the halo orbit of the valence nucleon, this also implied that a careful treatment of the form factor for transfer was required [14,15]. The form factor, or in other words the dependence of the transfer probability on the radial variable, is not an issue in knockout reactions because it is clear that in that case the outer parts of the halo wavefunction give rise to the whole cross section. However, the possibility of multistep reactions is an issue for knockout just as it is for transfer, in principle. In fact, transfer with a light, deformed halo nucleus is exceptionally complicated theoretically (see also ref. [16]) and it is encouraging that the results in the  $^{11}\text{Be}$  case [14,15] could be interpreted reliably.

Heavy ion induced transfer has also begun to be used, and at Oak Ridge the reactions ( $^{13}\text{C},^{12}\text{C}$ ) and ( $^9\text{Be},^8\text{Be}$ ) have been compared using targets of  $^{13}\text{C}$  and  $^9\text{Be}$  with a radioactive  $^{134}\text{Te}$  beam and clear  $j = \ell \pm 1/2$  selectivity was observed [17].

## What is different when using radioactive beams

The key difference, experimentally, when using radioactive beams (apart from the much lower beam intensity, of course) is that the kinematics are inverted, so that typically the lighter particle is the target. For heavy ion induced transfer, this means that the target-like particle may be very difficult to observe, since it may not escape from the target. For light ion induced reactions, the light target-like particle will typically escape from the target, and hence the experimenter has a choice of observing the beam-like particle, the target-like particle, or both. In the  $^{56}\text{Ni}(d,p)^{57}\text{Ni}$  example given above [13], the beam-like particle was detected as a tag of the correct reaction and the energy-angle systematics of the light, target-like particle were exploited to identify different excited states in  $^{57}\text{Ni}$ . In the  $^{11}\text{Be}(d,p)^{10}\text{Be}$  example [14,15] the approach was almost the opposite: the target-like particle was used as a tag and the energy and angle of the beam-like particle were analysed to isolate states in  $^{10}\text{Be}$  and measure their angular distributions.

The advantages and disadvantages of the various different approaches to light-ion induced transfer have been analysed in some detail [18] and summarised elsewhere [19,20]. In brief, the main difficulty with detecting the target-like particle is that rather a large angular coverage is required for the detection system. If detecting the beam-like particle, the kinematic focussing is into a small solid angle and a high resolution magnetic spectrometer can be used. The problem here is that exceptional resolution in angle is required, which is attainable for light beams, but which gets progressively more difficult as the mass and energy of the beam are increased. In either case, the resolution in excitation energy for excited states is limited (at least for practical target thicknesses, and the focussing conditions generally expected for radioactive beams) to several hundred keV. Active targets may help to overcome this, but for a conventional passive target it is more-or-less required that gamma-ray coincidence data be collected, if better resolutions are to be achieved.

Considering specifically light-ion induced transfer, the kinematical focussing of reaction products can easily be seen to be characteristic of the transfer type [19,20]. That is, for reactions such as (p,d) or (d,t) or (d, $^3\text{He}$ ) in inverse kinematics, where the radioactive projectile loses a neutron or proton, the light target-like ejectiles are confined to come out within a cone of forward angles in the laboratory frame. Furthermore, elastic scattering will always produce target-like ejectiles close to  $90^\circ$  and reactions such as (d,p) will have the target-like ejectiles distributed over the whole range of angles but with backward angles near  $180^\circ$  in the laboratory being of particular interest. The beam-like particles, for which the mass hardly changes with the transfer, are hardly deflected by the collision with such a light target and are found within a few degrees of the incident beam direction, as would intuitively be expected. It is the significant change in mass of the target-like particle that turns out to be the dominant effect in producing the characteristic kinematics. In the centre-of-mass frame, the light recoil has to compensate the momentum of the beam-like ejectile. Since the mass and velocity of the heavy particle are hardly changed by the transfer, the centre-of-mass velocity of the light recoil has to change dramatically in proportion to its dramatic percentage change in mass. The velocity observed in the laboratory frame will be the resultant sum of this centre-of-mass velocity of the light particle and

the velocity of the centre of mass in the laboratory frame. Details are given elsewhere [19,20] but basically the ratio of these two vector lengths is dominated by a factor  $\sqrt{f} = \sqrt{m_{target} / m_{ejectile}}$  related to the masses of the light particles before and after the transfer. For a reaction such as (p,d) or (d,<sup>3</sup>He) where  $f < 1$ , the velocity of the centre of mass dominates and focusses the light products into the forward hemisphere, typically forward of 40°. Of the two kinematic solutions at each forward angle, it is the one with the lower energy for the light particle that corresponds to small-angle scattering in the centre-of-mass frame. Normally, in a transfer reaction, this will be the solution with the higher yield. For a reaction such as (d,p) where  $f > 1$ , the velocity of the light ejectile will overcome the focussing effect of the moving centre of mass, and reaction products corresponding to small scattering angles in the centre-of-mass frame will emerge at backward angles in the laboratory frame.

In addition to these simple considerations of the important angular ranges, the mapping of the solid angle in three dimensions between the centre-of-mass and laboratory frames is also relevant to experimental design. In the case of (d,p) reactions, the formula describing this solid angle mapping [21] implies that coverage of the extreme backmost angles is not vital. In this region, the centre-of-mass angle changes so rapidly with laboratory angle that the effective solid angle is very small and both the yield and the structure in the angular distribution are only slight in the backmost 10° in the laboratory frame. However, it emerges that the whole range of angles between 170° and 90° should ideally be covered with good efficiency.

Finally, as long as the transferred mass is small compared to the projectile mass, it turns out that the energy-angle systematics of the light, target-like particle in inverse kinematics have little dependence on the precise mass or velocity (or MeV/A) of the incident beam particles. Combining all of the above information, it can be seen that a dedicated charged particle array can be designed, which will have wide applicability in the study of transfer reactions.

## DESCRIPTION OF THE TIARA DETECTOR ARRAY

The TIARA array of silicon strip detectors has been designed for transfer studies, to give accurate position information for charged particles over a solid angle of  $\approx 4\pi$ . In addition, it is extremely compact, so that gamma-ray detectors can be mounted in close geometry and hence have a high absolute efficiency. The compact design also allows for a magnetic spectrometer to be coupled at zero degrees and for beam tracking detectors to precede the target.

The detector arrangement in the first implementation of TIARA at GANIL, which is described here, differs slightly from the original design [22] in the forward angle region. It was decided to use a staged system of two concentrically mounted single-wafer annular detectors. These detectors are each divided lithographically to have 16 annular rings and 16 azimuthal sectors. Furthest from the target, at 150mm, one annular detector spans the angular range from 3.8° to 13.1°. The very outer part of that detector is actually obscured because the second detector is mounted at 90mm from

the target and spans angles from  $12.8^\circ$  to  $28.1^\circ$ . The barrel spans the angular range from  $35.6 \pm 0.4^\circ$  to  $143.4 \pm 0.4^\circ$  (where the errors indicate the variations due to the octagonal shape). In accordance with the original design, the backward angle region is spanned by an array of 6 wedge-shaped strip detectors, covering angles from  $137^\circ$  to  $169.4^\circ$ . Here, there are a total of 16 different annular bins of about  $2^\circ$  each, and 48 different azimuthal strips. The gap at forward angles, between  $28^\circ$  and  $35^\circ$ , will be filled in the near future.

Apart from the barrel, all other detectors are of a standard double-sided strip design. By combining information from the annular strips on the target side, and the azimuthal strips on the back, the pixel of the hit can be deduced. So far, no attempt at particle identification or time-of-flight has been implemented; just the angle and the deposited energy are recorded. In the backward-angle array, the full energy of the particle will be recorded, but at more forward angles the particles may often punch through and deposit a  $\Delta E$  signal in the silicon. All back-angle and barrel detectors are  $400 \mu\text{m}$  thick, being fabricated using 6-inch wafer technology [23], whilst the forward-angle detectors are  $500 \mu\text{m}$  thick. For the future, thicker detectors are actively being studied.

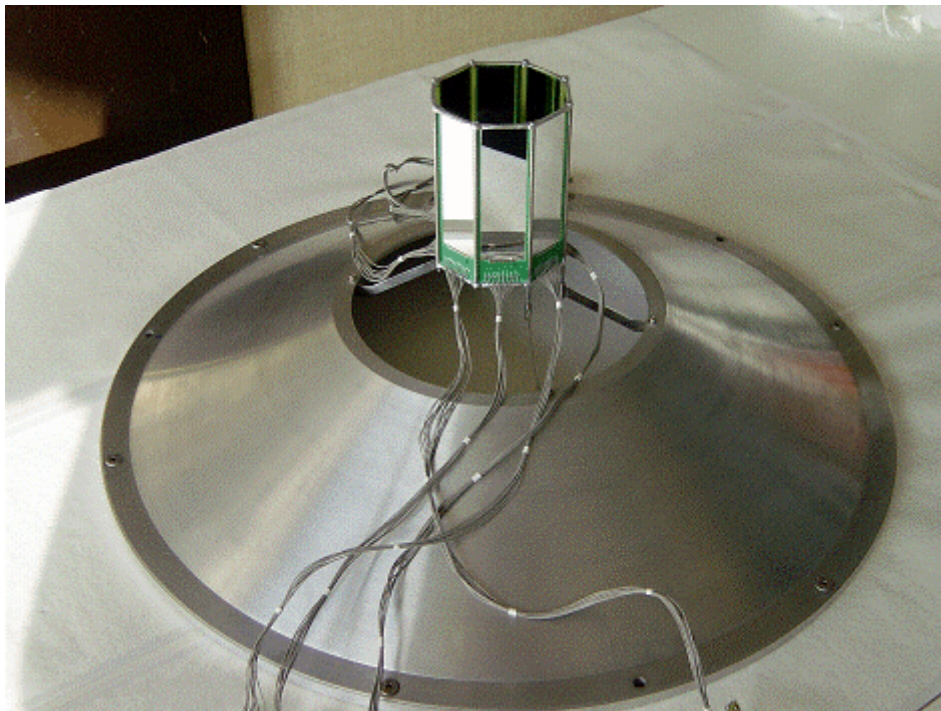


**FIGURE 1.** The fully assembled barrel of TIARA with its forward angle support structure.

The range of angles from  $35.6^\circ$  to  $143.4^\circ$ , as mentioned, is covered by the barrel part of TIARA. This comprises 8 individual detectors of length  $96.8\text{mm}$  and width  $24.6\text{mm}$ , each mounted on its own printed circuit board and then assembled into an octagonal barrel (see Fig. 1). Each detector in the barrel has 4 lengthwise resistive strips to measure the scattering angle. By means of tracks laid on both the silicon and the double-sided circuit board, all signals from both ends of the strips and from the back of the detector are brought out to connections at the forward-angle end of the

barrel. As shown in Fig. 1, the connections are then made by directly joining micro-coaxial cable to the circuit board, which is due to geometrical constraints. In the azimuthal direction, the position resolution is given by the strip width of 5.6mm or in angular terms ( $360/32=$ )  $11.25^\circ$ . For transfer, this is not important. In the longitudinal direction, the angular measurement depends on combining signals from the resistive strips. At present, the deposited energy is determined by adding the signals taken from each end of a given strip, and the position is determined by the difference of the signals. Thus, preamplifiers are connected to each end of each strip, which gives particular electronic properties described in the literature (see [24] and refs. therein). The position resolution has been measured to be  $< 1\text{mm}$  FWHM using a 5.5 MeV  $\alpha$ -particle source. This is shown in Fig. 2, where the observed image of a narrow slit is shown together with various fits; the best fit was derived by convolving a gaussian of 0.5mm FWHM with the projected geometrical image. The position resolution for this type of detector improves as the deposited energy is increased [24]. The energy resolution obtained by adding the signals from the two ends is 120 keV FWHM, and in fact slightly better resolution of 110 keV is obtained by directly taking the signal from the back face of the detector. These figures are typical for this type of detector and are small compared with resolution contributions expected to arise in reaction data due to target thickness effects.

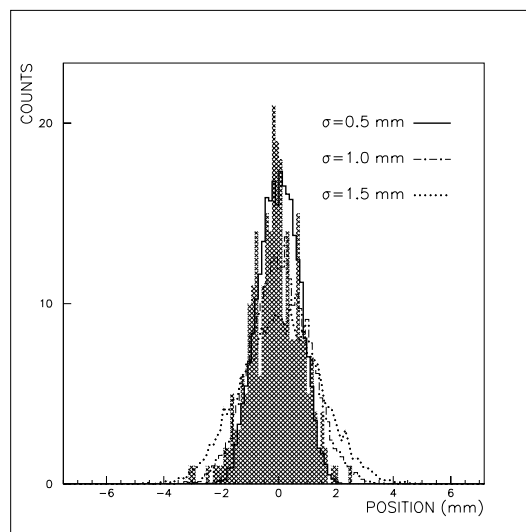


**FIGURE 2.** A position resolution of  $< 1\text{mm}$  FWHM measured in the resistive strips with  $^{241}\text{Am}$ .

## IMPLEMENTATION WITH OTHER DETECTORS

TIARA can operate as a stand-alone device, or just with gamma-ray detectors, but it is advantageous also to couple a magnetic spectrometer to separate or identify reaction products and un-reacted beam particles. In its first implementation at GANIL, the TIARA array is coupled with four gamma-ray detectors from the EXOGAM array and also with the VAMOS magnetic spectrometer, as described in the following.

## **The EXOGAM gamma-ray array**

The EXOGAM array [25,26] was designed specifically for experiments with radioactive beams. Each “clover” detector comprises 4 separate, tapered Ge crystals with a common cryostat, and then each Ge “leaf” is segmented electrically by means of 4 outer, corner contacts. These outer contacts can be used to infer in which quarter of the crystal the first interaction took place, for a given  $\gamma$ -ray. A separate, central contact in each crystal gives higher resolution energy information. The EXOGAM detectors are designed with symmetric  $45^\circ$  tapers on all edges, so that 18 detectors could be put together to make a complete sphere. With TIARA, either a complete octagonal ring of 8 detectors at  $90^\circ$  can be used or, as presently installed, a compact cube of 4 detectors centered at  $90^\circ$  and touching at their front edges, covering  $2/3$  of  $4\pi$  at a distance of 50mm from the target. The absolute full-energy peak efficiency at 1 MeV is around 20%. In this compact configuration, only certain escape-suppression shields at the rear and sides can be mounted, but for low  $\gamma$ -ray multiplicities this is not a significant limitation. The segmentation information allows a correction to be applied for the Doppler shift of  $\gamma$ -rays emitted by beam-like particles travelling along the beam axis. The relatively high velocities of the particles mean that the Doppler broadening, due to the finite geometrical acceptance of the detector, is what limits the  $\gamma$ -ray energy resolution. Depending on the energy, a resolution of order 50 keV is expected, which represents an order of magnitude improvement in excitation energy resolution relative to that achievable using charged particle energies and angles alone.

## **The VAMOS magnetic spectrometer**

The VAMOS spectrometer (“variable mode spectrometer”) is installed at GANIL for experiments with either fragmentation beams or ISOL beams from SPIRAL. It consists [27] of a pair of large-bore quadrupoles at the entrance, followed by an optional electrostatic section to give a Wien filter mode and then an optional dipole. At present, as set up with TIARA, it is operated using the quadrupoles and dipole. It has reasonable first-order focussing, a dispersion of  $25\text{mm}/\% \delta p/p$  and a momentum bite of close to 10%. These properties are suitable for transfer reaction studies in inverse kinematics. The large angular acceptance of  $\pm 10^\circ$  is not strictly needed, and indeed the silicon array is set up to detect smaller angles than this and therefore limits the acceptance into the spectrometer. VAMOS is designed for aberrations to be removed in software using fitted parameters, and this can be done on-line to recover the in-plane and out-of-plane entrance angles and the momentum. A physical beam-stop finger can be moved across the focal plane region so as to intercept the direct beam. This finger is made from plastic scintillator and can monitor and count the intense group that it intercepts.

## **The merging of the three separate data acquisition systems**

The master trigger signal for a transfer experiment with TIARA is produced whenever any strip in any silicon detector records a signal. This signal is produced



sufficiently quickly that it can also be included in the fast-trigger logic of EXOGAM and VAMOS. Each of these three data acquisition (DAQ) systems is thus enabled by a charged particle in TIARA. The TIARA system also includes an event counter in a VXI module called Centrum. When the EXOGAM and VAMOS DAQs record an internal trigger in overlap with the master trigger from TIARA, their slave Centrum units request the contents of the event counter kept in TIARA's master Centrum. The events from the three separate DAQs then include this event number and are broadcast in buffers independently onto a local data network, addressed to a processor that reads the buffers. A programme then correlates events, according to the event number, and builds combined events. These combined events are re-broadcast to a tape-server machine for storage. The combined data stream can also be sampled and analysed by on-line sorting programmes. The Centrum hardware units and the software for the on-line combination of the different data streams were developed by the GANIL data acquisition group. The method was developed and first implemented during the beam tests and commissioning of the TIARA array. Figure 3 shows how the three pieces of apparatus and DAQs are physically distributed around the beam area but connected by computer networks. Note that time-stamping, as shown in the figure, can be used instead of "stamping" events with the event counter. The key feature is that the final data as stored on tape includes all parameters from all acquisition systems in a single event structure for each trigger that is processed.

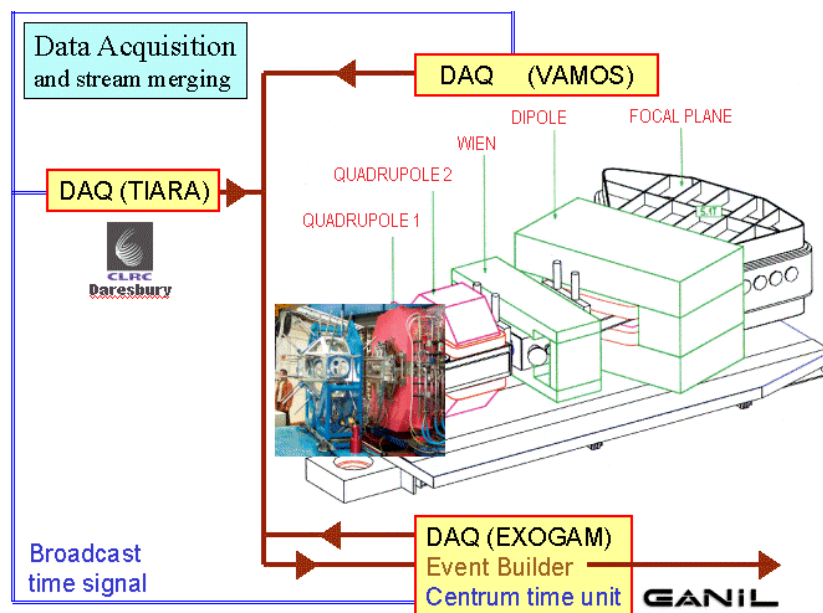


**FIGURE 3.** Three different data acquisition systems are merged on-line, using event stamping.

## COMMISSIONING AND FIRST EXPERIMENTS AT GANIL

TIARA has been successfully commissioned using the full silicon array described here, with 4 EXOGAM detectors and VAMOS. Commissioning runs were performed from June 2003 using beams of  $^{20}\text{Ne}$ ,  $^{36}\text{S}$  and  $^{14}\text{N}$  from the CIME cyclotron, to initiate

scattering and transfer on normal and deuterated polyethylene (CH<sub>2</sub>)<sub>n</sub> targets. The first experiment with a radioactive beam from SPIRAL was performed in September 2003 to study the reactions  $^{24}\text{Ne}(d,^3\text{He})^{23}\text{F}$  and  $^{24}\text{Ne}(d,p)^{25}\text{Ne}$  in inverse kinematics. The analysis of these data is in progress.

## ACKNOWLEDGMENTS

The TIARA project is the work of many people, including further collaborators at our own institutions. We wish also to acknowledge important input from Nigel Orr at LPC, Caen, France, our collaborators at Birmingham and Liverpool, UK, Christophe Theisen at Saclay, and our collaborators at GANIL, especially Hervé Savajols and Maurycy Rejmund. The development and construction of TIARA was funded by the EPSRC(UK) and the installation and commissioning was supported also by GANIL.

## REFERENCES

1. Austern, N., *Direct Nuclear Reaction Theories*, New York: John Wiley, 1970.
2. Satchler, G. R., *Direct Nuclear Reactions*, Oxford: Oxford University Press, 1983.
3. Glendenning, N., "One- and Two-Nucleon Transfer Reactions" in *Nuclear Spectroscopy and Reactions*, Part D, edited by J. Cerny, New York: Academic Press, 1975, pp. 319-344
4. Macfarlane, M. and Schiffer, J., "Transfer Reactions" in *Nuclear Spectroscopy and Reactions*, Part B, edited by J. Cerny, New York: Academic Press, 1975, pp. 169-194
5. Bond, P. D., *Phys. Rev* **C22**, 1539 (1980).
6. Anyas-Weiss, N. et al., *Phys. Reports* **12**, 201-272 (1974).
7. Catford, W. N., Fifield, L. K., Orr, N. A. and Woods, C. L., *Nucl. Phys.* **A503**, 263-284 (1989).
8. Hansen, P. G., *Phys. Rev. Lett.* **77**, 1016 (1996).
9. Hansen, P. G. and Sherrill, B., *Nucl. Phys.* **A693**, 133 (2001).
10. Sauvan, E., et al., *Phys. Lett.* **B491**, 1-7 (2000).
11. Bohr, A., and Mottelson, B. R., *Nuclear Structure*, Vols. 1 and 2, Singapore: World Scientific, 1997 (original editions New York: W. A. Benjamin Inc., 1969 and 1975).
12. Elbeck, B., and Tjorn, O., *Adv. Nucl. Phys.* **3**, 259 (1969).
13. Rehm, K. E., et al., *Phys. Rev. Lett.* **80**, 676-679 (1998).
14. Fortier, S., et al., *Phys. Lett.* **461B**, 22-27 (1999).
15. Winfield, J. S., et al., *Nucl. Phys.* **A683**, 48-78 (2001).
16. Timofeyuk, N. K., and Johnson, R. C., *Phys. Rev.* **C59**, 1545-1554 (1999).
17. Liang, F., Radford, D., et al., K., Oak Ridge National Laboratory, private communication.
18. Winfield, J. S., Catford, W. N. and Orr, N. A., *Nucl. Instr. and Meth.* **A396**, 147-164 (1997).
19. Catford, W. N., *Acta Phys. Pol.* **B32**, 1049-1060 (2001).
20. Catford, W. N., *Nucl. Phys.* **A701**, 1-6 (2002).
21. Schiff, L. I., *Quantum Mechanics*, third edition, New York: McGraw Hill, 1968, p. 113.
22. Catford, W. N., Timis, C.N., Labiche, M., Lemmon, R.C., Moores, G. and Chapman, R., in *Application of Accelerators in Research and Industry 2002*, edited by J.L. Duggan and I.L. Morgan, AIP Conference Proceedings 680, New York: American Institute of Physics, 2003, pp. 329-332.
23. Micron Semiconductor Ltd., Lancing, Sussex, UK.
24. Yanagimachi, T., et al., *Nucl. Instr. and Meth.* **A275**, 307 (1989).
25. Catford, W. N., *J. Phys. (London)* **G24**, 1337 (1998).
26. Simpson, J., et al., *Acta Physica Hungaria: Heavy Ions* **11**, 159 (2000).
27. Savajols, H., et al., *Nucl. Phys.* **A654**, 1027c (1999).